Feedforward and Feedback Connections and Their Relation to the CytOx Modules of V2 in *Cebus* Monkeys

Sheila Nascimento-Silva,[1] Carmen Pinõn,[1,2,3] Juliana G.M. Soares,[1] and Ricardo Gattass[1]*

[1]Institute of Biophysics Carlos Chagas Filho, Federal University of Rio de Janeiro, Rio de Janeiro, RJ, 21949-900, Brazil
[2]Faculty of Health and Life Sciences, Oxford Brookes University, Oxford OX3 0BP, United Kingdom
[3]Department of Experimental Psychology, The University of Oxford, Oxford OX1 3UD, United Kingdom

ABSTRACT

To study the circuitry related to the ventral stream of visual information processing and its relation to the cytochrome oxidase (CytOx) modules in visual area V2, we injected anterograde and retrograde cholera toxin subunit B (CTb) tracer into nine sites in area V4 in five *Cebus apella* monkeys. The injection site locations ranged from 2° to 10° eccentricity in the lower visual field representation of V4. Alternate cortical sections, cut tangentially to the pial surface or in the coronal plane, were stained for CTb immunocytochemistry or for CytOx histochemistry or for Nissl. Our results indicate that the V4-projecting cells and terminal-like labeling were located in interstripes and thin CytOx-rich stripes and avoided the CytOx-rich thick stripes in V2. The feedforward projecting cell bodies in V2 were primarily located in the supragranular layers and sparsely located in the infragranular layers, whereas the feedback projections (i.e., the terminal-like labels) were located in the supra- and infragranular layers. V4 injections of CTb resulted in labeling of the thin stripes and interstripes of V2 and provided an efficient method of distinguishing the V2 modules that were related to the ventral stream from the CytOx-rich thick stripes, related to the dorsal stream. In V2, there was a significant heterogeneity in the distribution of projections: feedforward projections were located in CytOx-rich thin stripes and in the CytOx-poor interstripes, whereas the feedback projections were more abundant in the thin stripes than in the interstripes. J. Comp. Neurol. 522:3091–3105, 2014.

INDEXING TERMS: primates; extrastriate cortex; cytochrome oxidase modules

The cortical visual areas are defined by the nature of their topographical representation of the visual field and their patterns of interconnections with other visual areas. Ungerleider and Mishkin (1982) proposed that the cortical visual areas of primates can be segregated into two functional streams of visual information processing. The dorsal stream projects to the parietal cortex and processes the movement and spatial relationships of objects. The occipitotemporal cortical pathway (i.e., the ventral stream) processes visual information about the shape, texture, and color of objects and is important for visual recognition in primates (DeYoe and Van Essen, 1985; Livingstone and Hubel, 1984).

The cytochrome oxidase (CytOx) modules in area V2 are comprised of CytOx-rich (thin and thick stripes) and CytOx-poor (interstripes) bands, have different neuronal properties, and participate differentially in these parallel channels by receiving information from modules in V1 and transmitting segregated information to specific extrastriate cortical areas (Wong-Riley and Carroll, 1984; De Yoe and Van Essen, 1985; Gattass et al., 1985, 1990, 1997; Zeki and Shipp, 1989; Sousa et al., 1991; Nakamura et al., 1993; Levitt et al., 1994;

Grant sponsor: The Brazilian National Council for Scientific and Technological Development (CNPq-47.1166/2013-8); Grant sponsor: Fundação Carlos Chagas Filho de Amparo à Pesquisa do Estado do Rio de Janeiro (FAPERJ-E-26/110.905-2013).

*CORRESPONDENCE TO: Ricardo Gattass, Ph.D., Programa de Neurobiologia, Instituto de Biofísica Carlos Chagas Filho, Bloco G, CCS, UFRJ, Ilha do Fundão, Rio de Janeiro, RJ, 21941-902, Brasil.
E-mail: rgattass@gmail.com

Received October 4, 2013; Revised December 6, 2013;
Accepted February 26, 2014.
DOI 10.1002/cne.23571
Published online March 1, 2014 in Wiley Online Library (wileyonlinelibrary.com)

Federer et al., 2009). Livingstone and Hubel (1984, 1987) showed that cells in the thin stripes of V2 have properties similar to those of the V1 blobs to which they are connected; these cells are mainly color-coding and non-orientation–selective. Likewise, cells in the interstripes of V2 have properties that are similar to those of the cells in the interblobs, which are orientation-selective. Cells in the thick stripes receive inputs from layer IVB of V1 and respond to depth cues and to moving stimuli. Lu et al. (2010) found robust direction maps, which exhibited pinwheel or linear organizations, in V2 thick/pale stripes that avoided thin stripes.

Additionally, it has been shown that the middle temporal area (MT) of the dorsal stream receives projections from the thick stripes, whereas areas of the ventral stream, such as V4 and TEO, receive projections mainly from the thin stripes and interstripe regions of V2 (DeYoe and Van Essen, 1985; Desimone et al., 1985, 1992; Shipp and Zeki, 1985, 1989; Desimone and Schein, 1987; Krubitzer and Kaas, 1990; Schein and Desimone, 1990; Van Essen et al., 1991; Nakamura et al., 1993; Levitt et al., 1994; Felleman et al., 1997; Nascimento-Silva et al., 2003).

Recent studies in macaque monkeys have reported an intermingling of visual information in these streams. Sincich and Horton (2005) found that interpatch neurons in layer II/III dominated the projections to thick as well as to pale stripes, and those 4B neurons, aligned in columns beneath the layer II/III clusters, also contributed substantially to both stripes (Sincich et al., 2010). Using rabies virus for transneuronal tracing, Nassi and collaborators (Nassi and Callaway, 2006; Nassi et al., 2006) revealed disynaptic inputs from the parvocellular lateral geniculate nucleus (LGN) to area MT. Ninomiya et al. (2011) found that V4 receives both magnocellular and parvocellular inputs through a trisynaptic pathway from layer IVC via layer II/III of V1 and a disynaptic input from the thick stripes of V2 via the thin stripes and/or the interstripes.

This result implies that pale and thick stripes receive the same input from V1, rather than different messages concerned with form and stereo/motion, respectively. An et al. (2012) found that the orientation domains in macaque V1, V2, and V4 also served to process motion signals associated with the axis and speed of motion. In contrast, direction domains within the thick stripes of V2 demonstrated preferences that were independent of motion speed. More recently, Li et al. (2013) found that V4 contains direction-preferring domains that are preferentially activated by stimuli moving in one direction. These direction-preferring domains normally occupy several restricted regions of V4 and tend to overlap with orientation- and color-preferring domains. Single-cell recordings targeting these direction-preferring domains also showed a clustering, as well as a columnar, organization of V4 direction-selective neurons. These data suggest that, in contrast to the classical view, motion information is also processed in ventral pathway regions such as area V4.

The laminar distributions of labeled cells and terminals have been used as criteria for distinguishing feedforward projections, which originate from cells in the superficial layers and mostly terminate in layer IV of a higher order target area, from feedback projections, which originate from cells in the infragranular layers and mostly terminate outside of layer IV of lower order target areas and have been used to build a hierarchical model of extrastriate cortex. However apparent, this laminar segregation of ascending and descending inputs is not absolute or can be complicated, in part due to the presence of translaminar intrinsic axons and dendrites (Spatz and Tigges, 1972; Rockland and Pandya, 1979; Maunsell and Van Essen, 1983; Weller and Kaas, 1985; Ungerleider and Desimone, 1986; Boussaoud et al., 1991; Felleman and Van Essen, 1991; Shipp et al., 2009; Markov et al., 2014). It becomes vital to fully understand feedforward and feedback connectivity between V4 and other areas such as V2 and how this might contribute to an understanding of the hierarchical structural organization of the visual cortex.

Over the past 30 years, we have been studying the visual system of the New World *Cebus* monkey as a model for the human visual system, replacing in many aspects the need for using Old World monkeys (Gattass et al., 1990). *Cebus apella* is a diurnal monkey with brain size and sulcal pattern similar to that of *Macaca fascicularis*. We propose that it serves as an adequate alternative model for study of the primate visual system. The aim of this study is to gather additional data about the modules of V2 and its connections with V4 in New World monkeys.

We have previously described the feedforward modular V2 projections to V4 in *Cebus* monkeys (Nascimento-Silva et al., 2003). Here, we were interested in determining how feedforward and feedback projections are distributed through the cortical layers and organized in relation to the CytOx modules of V2. We used cholera toxin subunit B (CTb), which has been used as a bidirectional tracer to visualize cell soma and axon terminals (Angelluci et al., 1996). We report on the arrangement of projections in the region of the representation of the central lower field of V4, which links V2 and V4 in *C. apella*, in relation to the CytOx-rich and -poor modules of V2 and reveal the laminar and tangential distributions of the feedforward and feedback projections of V2. The use of injections of CTb into V4 allowed us to specifically label the V2 modules and

provided an efficient method for elucidating the modular circuitry of V2. The distributions of projections were significantly heterogeneous; feedforward projections originated in the thin stripes and interstripes (as did the feedback projections from V4) but were richer in the thin stripes than in the interstripes.

MATERIALS AND METHODS

All experimental protocols were conducted following NIH guidelines for animal research and were approved by the committee for animal care and use of the Institute of Biophysics Carlos Chagas Filho, Federal University of Rio de Janeiro.

Five adult *C. apella* monkeys ranging in weight from 2.8 to 4.0 kg were used. These animals were also used for other anatomical projects. Each animal was anesthetized with ketamine hydrochloride (30 mg.kg IM Ketalar; Parke-Davis, São Paulo, SP, Brazil) and received atropine (0.15 mg/kg IM Atropina; Hypofarma, Rio de Janeiro, RJ, Brazil) and benzodiazepine (0.5 mg/kg IM Valium; Roche, Rio de Janeiro, RJ, Brazil). Anesthesia was maintained with infusions of sodium thiopental (10 mg/kg/h IV Tiopental; Cristália, São Paulo, SP, Brazil) in 5% glucose or with regularly repeated IM injections of a 1:5 mixture of 6% ketamine hydrochloride and 2% dihydrotiazine hydrochloride (Rompun, Bayer, Rio de Janeiro, RJ, Brazil). Level of expired CO_2, rectal temperature, and heart rate were continuously monitored throughout the experiment and maintained within physiological ranges. A craniotomy was made over the intended injection sites under sterile conditions, and the dura mater was sectioned to expose the cortical surface. Injections were made under visual guidance. Following the injections, the wound was closed in anatomical layers, and the animals received IM injections of penicillin G (300,000 IU Benzetacil; Eurofarma, São Paulo, SP, Brazil).

Volumes ranging from 0.2 to 1 μl of 1% CTb (Sigma-Aldrich, St. Louis, MO) were injected into the cortical surface of the prelunate gyrus under direct observation using a 1-μl 27-gauge needle Hamilton (Reno, NV) syringe (Fig. 1). As a reference, we used the superficial blood vessel that runs over the superior temporal gyrus from the inferior occipital sulcus to the superior temporal sulcus. Injections were made into one or both hemispheres in each animal for a total of seven hemispheres.

We inferred the eccentricity of the injections based on the location of the back projections of V2, using the visuotopic map described by Rosa et al. (1988). The distance from the fovea of V2 to the projection was confronted with the intended location in V4, using the integration of the magnification factor function for V2.

After of 7–21 days of survival, the animals received lethal doses of sodium pentobarbital (90 mg/kg IV) and were transcardially perfused. Four animals underwent a flattening procedure, and the remaining animal was perfused, fixed, and cut in the coronal plane.

The four animals were perfused with 0.9% saline followed by 0.1 M phosphate buffer at a pH of 7.4. To obtain flattened cortical preparations for the first four animals, the brains were removed from the skull, and blocks that included areas V1, V2, and V4 were separated from the rest of the brain and then flattened. To separate the block, we cut along the posterior tip of the superior temporal sulcus (st), and the cortex was separated from the white matter from the st tip to the lunate sulcus (lu) superior and inferior to the occipital sulcus (io) below, which included part of area V4. Following the occipital operculum, the cortex was dissected along the fundus of the lu and the fundus of the io at the striate cortex far from the V1/V2 border to the large belt that included the dorsal parts of V3, V2, and V1. Next, this tissue block was gently unfolded and interposed between glass slides, pressed, and submersed in a fixation solution. This preparation was fixed with a solution of paraformaldehyde (4%) in 0.1 M phosphate buffer for 12 hours and then stored overnight in phosphate buffer/glycerol (10%). Frozen sections (60 μm) were cut in a plane tangential to the pia mater. Alternate sections were designated for CTb immunohistochemistry (Angelucci et al., 1996) or CytOx enzyme histochemistry, which was performed according to the modified Silverman and Tootell (1987) method.

The remaining animal was perfused with 0.9% saline followed by 4% paraformaldehyde in phosphate-buffered saline (PBS), 4% paraformaldehyde PBS with 2.5% glycerol, PBS with 5% glycerol, and PBS with 10% glycerol overnight. The next day, the brain was frozen and sectioned into 40-μm-thick coronal sections using a cryostat. Adjacent sections were stained for cell bodies using cresyl violet, CO histochemistry, or immunocytochemistry for CTb.

For immunocytochemical reactions, the sections were incubated overnight in a polyclonal cholera toxin antibody (1:1,500–2,000; Sigma-Aldrich) in a solution containing 0.05% bovine albumin and 0.3% Triton X-100 in 0.01 M PBS at a pH of 7.4. Sections were then incubated for an additional hour in biotinylated anti-rabbit secondary antibody and then processed by the avidin–biotin method with ABC kits (Vector, Burlingame, CA) and nickel-enhanced diaminobenzidine. The sections were rinsed in PBS, mounted on gelatin-coated slides, dehydrated, and coverslipped. Control sections were prepared by omitting the primary antibody in the incubation solution. These sections showed no specific staining.

CTb sections were scanned for the distribution of the labeled cells and terminals by using a Leitz (Wetzlar,

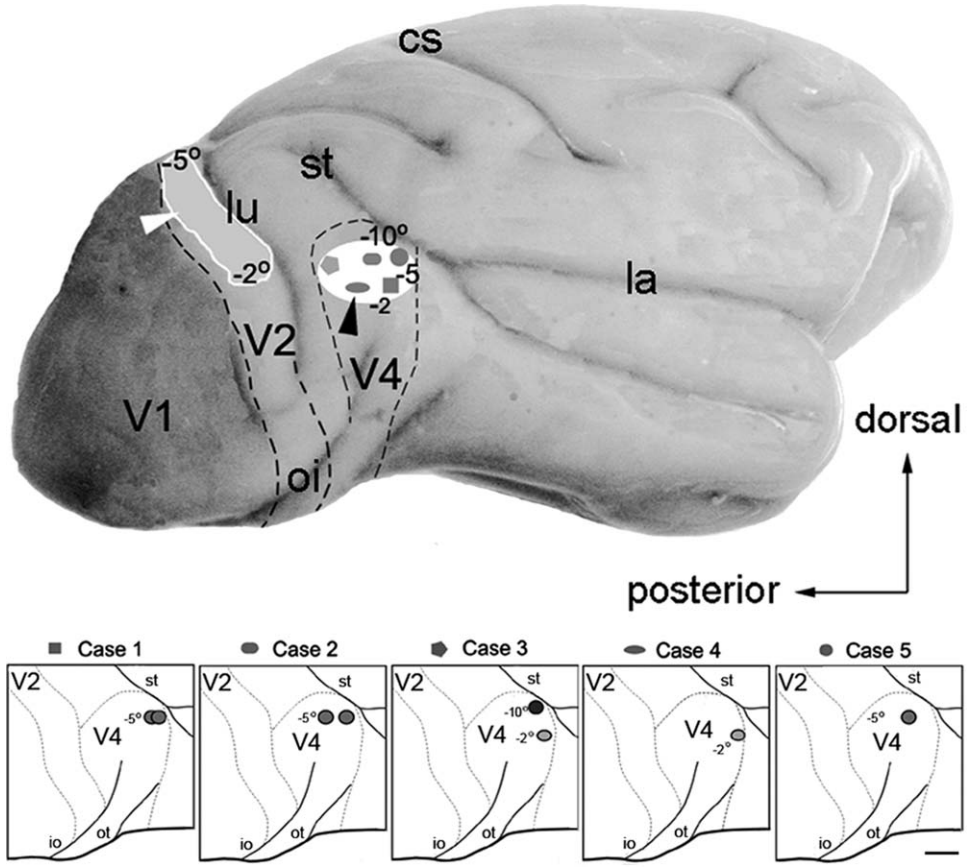

Figure 1. Injection sites in V4 in five cases. **Top:** Lateral view of the brain. The white box shows the extension of the injection sites in V4 from −2° to −10° of the representation of the lower visual field for each of the five cases; the projection sites in V2 extended from −2° to −10° in the lower visual field. (Projections beyond −5° were in the medial convexity of the brain.) Dashed lines represent the borders between areas. **Bottom:** Location of each injection relative to the sulci. Abbreviations: lu, lunate sulcus; io, inferior occipital sulcus; st, superior temporal sulcus; cs, central sulcus; la, lateral sulcus; ot, occipital temporal sulcus. Scale bar = 5 mm.

Germany) Diaplane microscope interfaced to a Minnesota Datamatrix X-Y system (A) or a Zeiss (Thornwood, NY) microscope interfaced to a Neurolucida system (B; MBF Bioscience, Williston, VT). The labeled neurons were plotted onto drawings of the sections' contours and photographed. Each section stained for CO was used for the reconstruction of the stripe pattern in V2. Labeled cells were projected onto the photographic reconstruction of the CO compartments of V2 to allow for analysis of the relationships of the labeled cells in V2 with the CO-modules using Adobe Photoshop (San Jose, CA). In the coronal sections, we used the adjacent Nissl sections to identify the layers in which the labeled cells and terminals were located. The contours of the sections, the layers, and the landmarks were drawn by using the Neurolucida system and then transferred to NeuroExplorer (Nex Technologies, Madison, AL) for data analysis.

We used Neurolucida to capture, align, and organize the sections used for the evaluation of cell and fiber density of all animals. The Neurolucida system was used to capture whole slide images from the entire sections (digital scans) and to make serial section reconstructions of V2 and surrounding areas. We used its tools to align the section and to obtain a final aligned serial section reconstruction for each animal. The serial section reconstructions of V2 were used to trace and analyze the CytOx bands and to segregate the cortical layers through multiple sections. After aligning the sections, we transferred the limits of the CytOx-rich label to the sections stained for CTb for quantification.

Quantification was done using all sections. Tangential sections were used for the analysis of width of CytOx band, and distribution of cells and fibers in these compartments. Oblique and coronal sections were used for both the analysis of the distribution in the compartments of V2 and also for distribution in the different layers.

We used coronal section series to draw the limits of the cortical layers by cytoarchitecture. In these series,

we determined the relative depth of these transitions of the cortical layers to use in other series stained for CytOx or CTb.

When 40-μm tangential sections are used, the depth of the sections is an indication of the cortical layer. Cutting from the pial surface to the white matter, section 1 corresponds to the top of layer I, whereas the last section (usually section 37) corresponds to the bottom of layer VI. When we had oblique sections identified by serial section reconstruction, we used these sections to study both the distribution of cells and fibers in the CytOx bands of V2 and the distribution in different cortical layers. For example, we selected oblique sections that were cut around layer IV at the V1/V2 border and would reach the pial surface (layer I) close to the anterior border of V2 to evaluate the distribution in both the CytOx band and the supragranular layers.

The cell counts of each compartment were determined by using Neurolucida. We used a MatLab (MathWorks, Natick, MA) density program to measure the optical density of fibers from images in slabs of predetermined sizes. CTb-stained sections were cut in rectangles of predetermined sizes (200 × 50 μm). MatLab measures the average optical density of individualized pixels. Densely stained clusters of pixels larger than 20 μm in diameters were not computed. This procedure avoids the interference of cell bodies in fiber density measurements. The measurements made in oblique sections were divided into larger rectangles.

Data from each section from each animal were used to feed a database (summarized in Figs. 8–11. The data were transferred to a Systat 8 file (Systat Software, Chicago, IL) for statistical analysis.

RESULTS

We analyzed data from nine CTb injections into area V4 in five animals. We will first present the connections of V4 with the CytOx modules in the flattened preparations of V2.The laminar distributions of labeled cells and terminals are described as the feedforward and feedback V2 projections from area V4. By analyzing the distributions of labeled cells and terminals in the coronal sections, we illustrate and quantify the laminar distribution of the labeling. We then describe the cell types and spatial organization of cells and terminals.

Injections of CTb in V4

Figure 1 shows the CTb injection sites in V4 for each of the five cases. Case 1 received two injections of 0.5 μl CTb into the dorsal part of V4 ranging from 2° to 5° eccentricity. Case 2 received two injections of 0.5 μl CTb in the dorsal part of V4 (5°). Case 3 received two injections of 1.0 μl CTb in the right hemisphere and one injection of 0.2 μl CTb in the left hemisphere; both injections were in the dorsal part of V4. One injection into the right hemisphere was located in the representation of the peripheral visual field (10°), and the other was located in the representation of the central lower visual field in V4 (2°). Case 4 received an injection of 0.2 μl CTb in the representation of the central lower visual field in V4 (2°). In both cases (i.e., cases 3 and 4), we detected similar labeling in V2; however, in case 3 (injection into the representation of the peripheral visual field), the tracer spread into area TEO, and the injection into the representation of the central visual field in the opposite hemisphere invaded the white matter. Case 5 received one injection of 0.5 μl CTb in the dorsal part of V4 in the representation of the pericentral lower visual field at 5° eccentricity. Coronal sections of the occipital cortex in front of the V1/V2 border and behind the lunate sulcus revealed regular arrangements of labeled cells and terminals in different cortical layers (Fig. 1).

Projections in V2

After injections of CTb into V4, labeled cells and terminals were located in the stripes perpendicular to the V1/V2 border in V2. The projections from 2° to 5° were located in dorsal lateral V2 (Fig. 1), whereas those from 6° to 10° eccentricity were located in dorsal medial portions of V2 (not shown). In all four cases, the flattened preparations of V2 showed clusters of projections that were organized into bands that were orthogonal to the V1/V2 border (Figs. 2 and 3).

Figure 2 shows the injection sites in V4 and the projections in V2 in the flattened sections of two animals (cases 1 and 2). The injections were restricted to visual area V4 and produced regularly spaced projections to V2 in both animals. These projections are composed of groups of cells and fibers that were clustered along bands that were orthogonal to the V1/V2 border. Outside V2, in V3, only one cluster was found in case 1.

The CTb-labeled patches of cells represent the origins of the feedforward projections to V4, whereas the terminals constituted feedback projections from V4 to V2.

Projections and CytOx modularity

Figure 3 shows the CytOx bands and CTb-labeled cells and terminals in V2 from case 3. These data allowed comparison of the locations of the CytOx bands of V2 with the patches of projections from V4. One CytOx-stained oblique section of V2 (Fig. 3A), a filtered montage of CytOx staining in layer IV from a set of

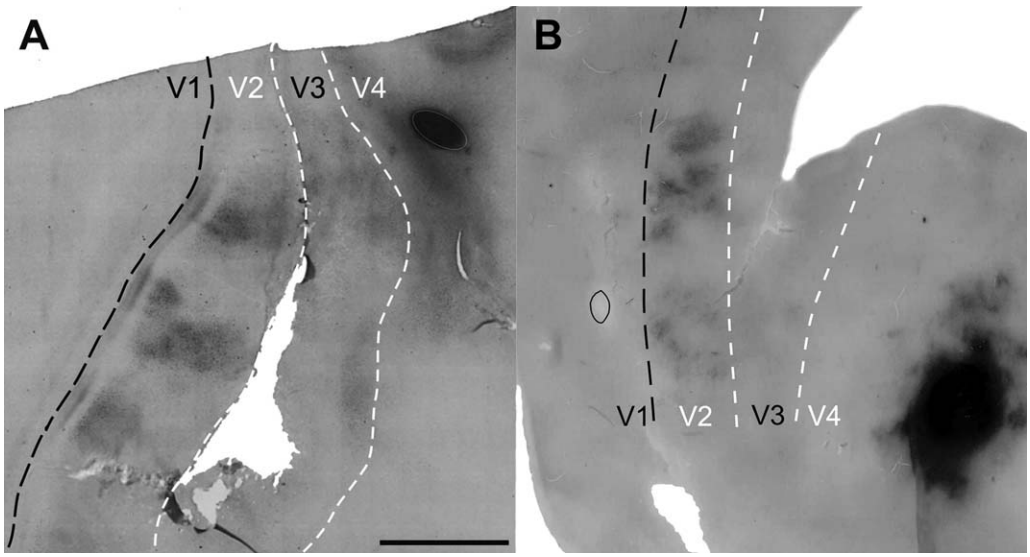

Figure 2. **A,B:** Injections in V4 and projections to V2 in the flattened sections of two cases (case 1, A and case 2, B). Groups of cells and fibers are regularly spaced in V2 in both animals. Injections restricted to the visual area V4 are shown to the right of the sections in each animal. Black dashed lines show the V1/V2 border. White dashed lines show the estimated V2/V3 and V3/V4 borders. Scale bar = 5 mm in A (applies to A,B).

neighboring sections (Fig. 3B), and an alternating neighboring CTb-stained section (Fig. 3C) show the correspondence of labeled cells and terminals with the CytOx-rich thin bands and the CytOx-poor interbands of V2. The montage (middle sections) was based on stacked segments of layer IV from neighboring CytOx-stained sections of V2. The collage (Fig. 4B) was filtered (Gaussian filter = 100 μm [30 pixels]) using Photoshop 7 to generate a pictorial representation of the bands of V2. The patches of CTb-stained cells and terminals in the upper layers of V2 were located in thin CytOx-rich modules and intermodules of V2. Lightly stained cells were clustered mainly in the upper layers, whereas dense fibers were clustered in the lower layers (Fig. 3C).

Figure 4 shows the clusters of labeled cells and terminals located in the supragranular layers II and III that corresponded to the CytOx-rich thin stripes and CytOx-poor interstripes in V2 after injections of CTb into V4 of case 3. No labeled cells were found in layers I and IV in V2 (Fig. 4). Most of the neurons were located in layer III, in the CytOx-rich thin stripes. The cells in this layer were larger than the labeled cells in others layers. The distribution in the infragranular layers was concentrated in layer VI. Strong labeling of terminals was found in the supragranular (layers I and II) and infragranular layers (bottom of layer V and layer VI) (Fig. 4).

Figure 5 shows CTb-stained cells and fibers from the thin CytOx–rich band and interbands in V2 of case 4. Low-power photomicrographs from sections of V2 stained for CTb (Fig. 5A, left) and CytOx (Fig. 5A right) show the correspondence of the location of the CytOx modules of V2 with the clusters of labeled cells and fibers. Figure 5B shows high-power photomicrographs obtained from subsequent tangential sections (10, 08, 06, and 02) with CTb-labeled cells and terminals. The overlay of these data shows that the CTb-labeled cells and terminals were related to one CytOx-rich thin stripe that was interposed by two CytOx-poor interstripes of V2 and extended approximately 2 mm, avoiding the thick stripes (Fig. 5A, right).Overall, the clusters of labeled cells appear to be distributed in the interbands and thin bands, although the terminal-like labeling appears to be restricted to interstripes. Thus, the clusters of cells that were in the thin bands and interbands avoided the domains of the thick CytOx-rich bands.

Laminar distribution of labeled cells and terminals in V2

Figure 6 shows the location of the CTb-labeled cells in the cortical layers of V2 in coronal sections from case 5. Nissl-stained (Fig. 6A) and neighboring CTb-immunoreacted sections (Fig. 6B and 6C) show that the labeled cells were mainly located in layer III and were sparsely located in layer V. In this figure, approximately 91% of the labeled cells were located in the supragranular layers, and 9% were located in the infragranular layers. The patches of labeled cells encompass approximately 600 μm, and they were separated by roughly 2 mm (Fig. 6B).

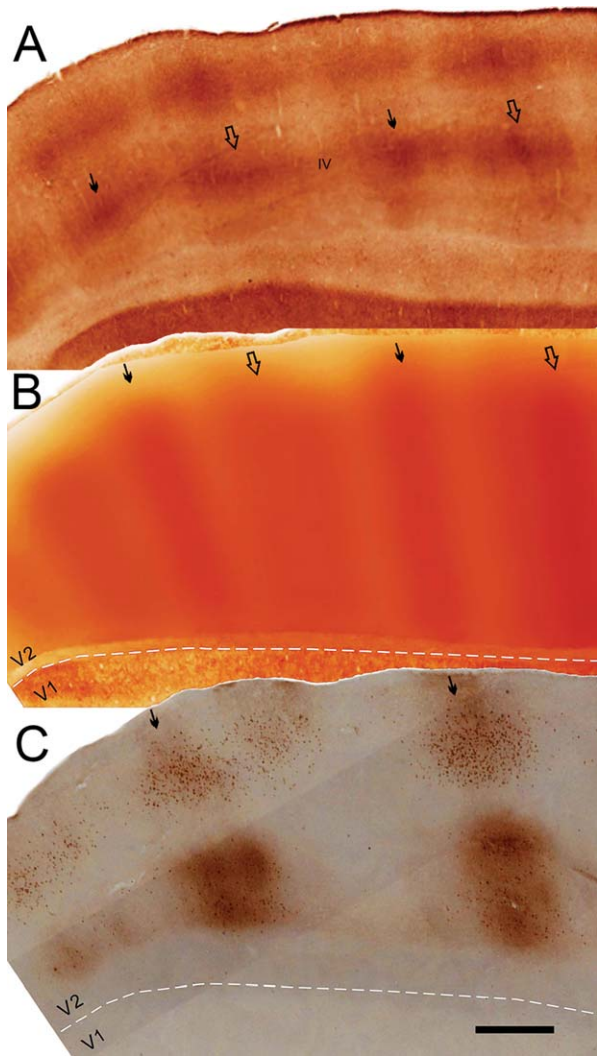

Figure 3. CytOx-bands and CTb-labeled cells and terminals in V2 from case 3. **A–C:** CytOx-stained oblique section of V2 (A), montage of layer IV of V2 from neighboring sections (B), and alternated neighboring CTb-stained sections (C) showing the corresponding locations of cells and terminals in relation to the CytOx-thin bands and interbands of V2. White dashed lines show the V1/V2 borders. Segments of layer IV of V2 from adjacent CytOx-stained sections were stacked together and filtered (Gaussian filter = 100 μm [30 pixels]) using Photoshop 7 to compose the montage shown in B. Cells and minimally dense CTb-staining are shown in clusters in the upper layers, and heavily dense fibers and cells are clustered in the lower layers. Thin solid arrows point to the location of thin CytOx-rich bands in B and C and in layer IV in A. Thick open arrows point to the location of thick CytOx-rich bands in B and C and in layer IV in A. Scale bar = 1 mm in C (applies to A–C).

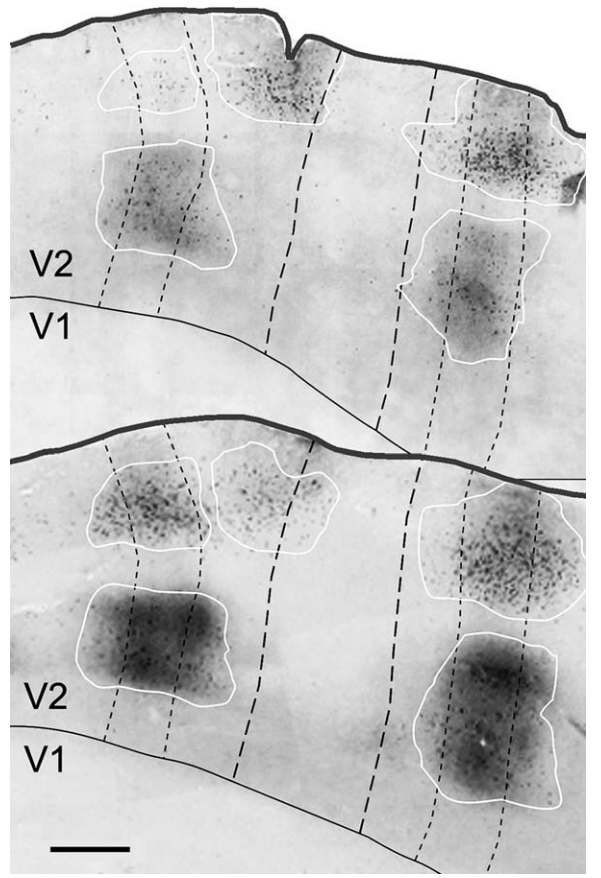

Figure 4. CTb-labeled cells and terminals in two oblique flattened V2 sections from case 3. Thin dashed lines outline the thin CytOx bands, and thick dashed lines outline the thick bands. White lines delineate the patches of CTb-labeled cells and terminals. Black lines show the V1/V2 borders. Scale bar = 1 mm.

Figure 7 shows the labeled cells and terminals in two enlarged bright- and darkfield photomicrographs of V2 after injections of CTb in V4 of case 1. The brightfield photomicrographs show the distribution of cells and fibers in different cortical layers of V2 (Fig. 7A). The darkfield photomicrograph emphasizes the distribution of labeled fibers in the infragranular layers of V2 (Fig. 7B). Figure 7B shows complex meshes of fibers in lower and upper layers and patchy vertical bundles of fibers at the thin CytOx-rich modules of V2. The cells predominantly occupied the supragranular layers, mainly layer III, whereas the terminals were located in the infragranular layers, particularly layer V.

The majority of labeled cells in area V2 were pyramidal cells with ascending vertical dendrites, and large stellate cells containing large nuclei composed a small population (Fig. 8A,D). These cells were densely organized in clusters in the thin stripes and sparsely organized in the interstripes. These clusters spread to one CytOx-rich thin stripe and one or two CytOx-poor interstripes in the flattened preparations. Figure 8D shows clusters of CTb-labeled cells in six enlarged microphotographs of flattened sections of V2.

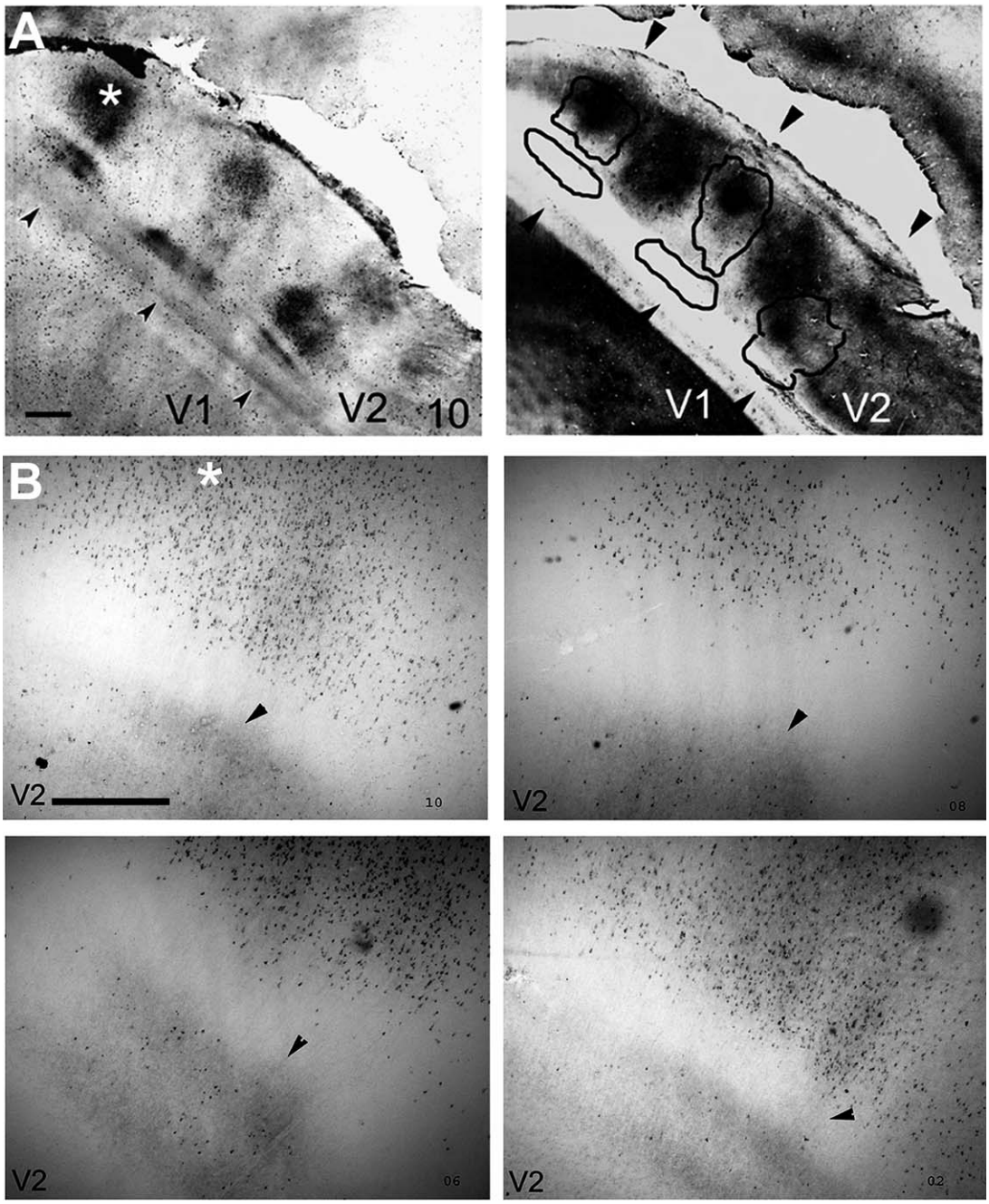

Figure 5. CTb-stained cells and fibers from the thin CytOx-rich band and inter-bands in V2 from Case 4. **A:** Low-power photomicrograph of section 10, showing V2 stained for CTb (left) and CyOx (right), with a CytOx-rich band of V2 (black lines). **B:** Enlarged photomicrographs obtained from adjacent tangential sections (10, 08, 06, and 02) showing CTb-labeled cells and terminals. The arrowheads mark blood vessels used to align the photomicrographs. The location of the high-power photomicrographs corresponds to the site marked with an asterisk on the left side of A. Scale bar = 1 mm in A and B.

Morphometric analyses

CytOx bands

To evaluate the correspondence of the locations of the patches and the CytOx modules of V2, we measured the width of the bands and interbands. Figure 9 shows the average width of the CytOx-rich thin and thick bands and CytOx-poor interbands of V2 in three animals. On average, the thin bands were 1,300 μm wide, and the thick bands were 1,600 μm wide. The interbands were, on average, 350 μm wide.

Laminar distribution

We also measured the number of cells in each cortical layer and in each CytOx compartment. Figure 10 shows

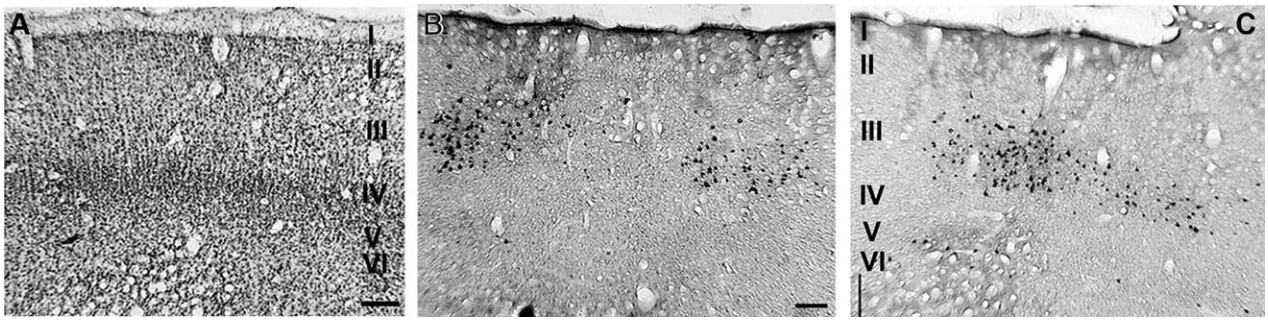

Figure 6. Locations of the CTb-labeled cells in the cortical layers of V2. **A–C:** Nissl-stained (A) and neighboring CTb-immunereacted parasagittal sections (B,C) showing the locations of labeled cells in layer III in case 5. Scale bar = 100 μm.

the relative frequency of labeled cells in each CytOx compartment and in cortical layers II, III, and V after injections of CTb into V4. Layer III had the greatest number of cells, followed by layer V, and very few cells were located in layer II. In every layer, there were more cells in the thin bands than in the interbands and very few cells in the thick bands.

Figure 11 shows the variations in the numbers of labeled cells and fiber densities throughout the cortical layers of V2 at the location of a set of modules composed of one CytOx-rich thin band and two CytOx-poor interbands of V2 after injections of CTb into V4. The density of labeled cells peaked in layer III (5 cells/mm^2), whereas the density of fibers was greatest in layer V.

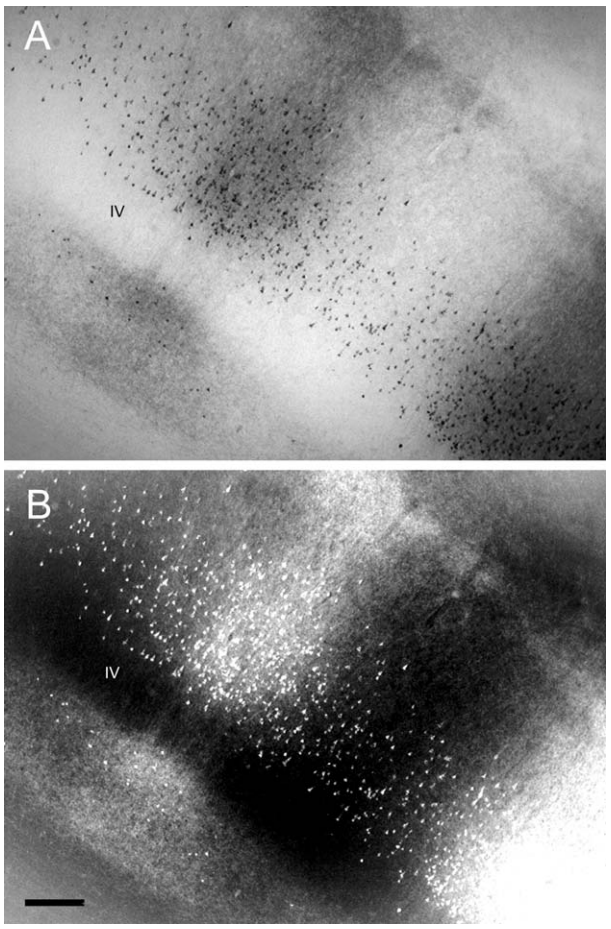

Figure 7. **A,B:** Brightfield (A) and darkfield (B) photomicrographs of labeled cells and fibers in V2 after an injection of CTb in V4 in case 1. Scale bar = 200 μm in B (applies to A,B).

DISCUSSION

CytOx modules and pathways

The occipitotemporal cortical pathway is called the ventral stream of visual processing and is necessary for visual recognition in monkeys (Ungerleider and Mishkin, 1982; Mishkin et al., 1983; Ungerleider, 1985; Maunsell and Newsome, 1987; Weller, 1988; Desimone and Ungerleider, 1989; Felleman and Van Essen, 1991; Van Essen et al., 1991, 1992). This pathway includes successively ordered areas that begin in the striate cortex (visual area V1), and project to the extrastriate visual areas V2 and V4, and then further on to the inferior temporal cortex (areas TEO and TE). Along this stream, the complexity of the physiological properties of neurons and their responses to the visual stimuli increase, and receptive field sizes also increase at each stage (Gross et al., 1972; Desimone and Gross, 1979; Gattass et al., 1981, 1988; Tanaka et al., 1991; Pasupathy and Connor, 1999; Orban, 2008). Kravitz et al. (2011) reviewed the anatomical and functional evidence in primates and suggested that the dorsal stream actually gives rise to three distinct, major pathways; a parieto-prefrontal pathway, a parieto-premotor pathway, and a parieto-medial temporal pathway.

Within at least the early stations of these pathways, there are functional modules that make differential

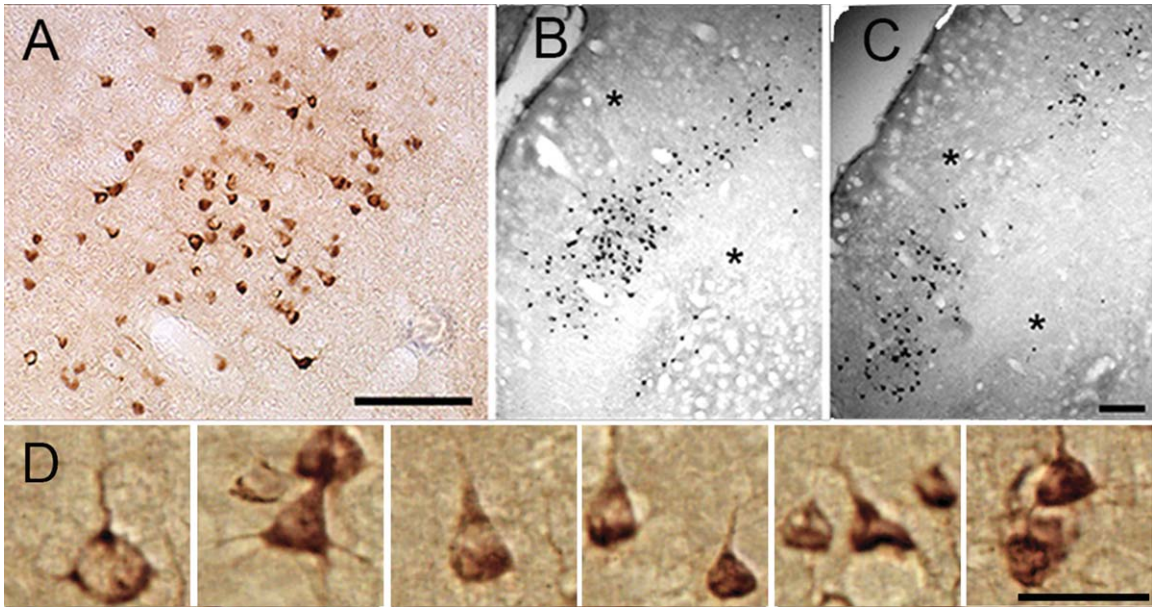

Figure 8. Types of cells that were CTb-labeled in oblique sections of V2. **A:** Enlarged colored photomicrograph of CTb-labeled cells in layer III in V2. **B,C:** CTb-immunoreacted sections showing clusters of labeled cells in the upper layers of V2. Asterisks indicate corresponding blood vessels. **D:** Cell types exhibiting feedforward projections in layer III of V2. Enlarged photomicrographs show the labeled cells in V2 after an injection of CTb in V4. Scale bar = 200 μm in A, C (applies to B,C), and D.

contributions to color, form, and motion processing. In V1 and V2, modules can be identified histologically in cytochrome oxidase (CO)-stained sections (Horton and Hubel, 1981; Livingstone and Hubel, 1982, 1984, 1987; Humphrey and Hendrickson, 1983; Tootell et al., 1983; Carroll and Wong-Riley, 1984; Horton, 1984; Wong-Riley and Carroll, 1984; DeYoe and Van Essen, 1985; Hubel and Livingstone, 1985, 1987; Shipp and Zeki, 1985, 1989; Cusick and Kaas, 1988; Zeki and Shipp, 1989; Gattass et al., 1990; Krubitzer and Kaas, 1990).

Area V2 has both thick and thin stripes of dense CO staining situated deep in layer III and layers IV and V, and both of these stripes are bordered by CO-poor interstripe regions. The CO-rich thin stripes of V2 receive inputs from the blobs of V1, the interstripe regions receive inputs from the interblob regions of V1, and the CO-rich thick stripes receive inputs from layer IVB of V1 (Livingstone and Hubel, 1984, 1987). However, Federer et al. (2013) have proposed that the pale stripes in V2 are anatomically two distinct compartments receiving different projections from layers II and III in V1, with only one set receiving a significant projection from layer 4B, whereas the other set receives few or no layer 4B projections. Consistent with these inputs, although the CO-dense stripes are not consistently distinguishable as thick or thin, they can be identified by functional differences, with neurons in the thick stripes sensitive to binocular disparities and stimulus orientation and direction, neurons in the thin stripes sensitive to luminance and color, and neurons in pale stripes sensitive to stimulus orientation (Livingstone and Hubel, 1984; DeYoe and Van Essen, 1985; Hubel and Livingstone, 1985, 1987; Shipp and Zeki, 1985; Lu and Roe, 2007, 2008; Felleman, 2008, Kaskan et al., 2009; Lim et al., 2009). Lu et al. (2010) found robust direction maps that exhibited pinwheel or linear organizations in V2 thick/pale stripes that avoided thin stripes. The presence of motion maps in V2 points to a newfound prominence of V2 in motion processing, for contributing to motion perception in the dorsal pathway and/or for form perception dependent of motion.

Area V4, which receives inputs from both CO-rich thin stripes and CO-poor interstripe regions of V2, has both color- and form-selective cells and many cells that are sensitive to both features (Desimone et al., 1985, 1992; DeYoe and Van Essen, 1985; Shipp and Zeki, 1985, 1989; Desimone and Schein, 1987; Zeki and Shipp, 1988, 1989; Schein and Desimone, 1990; DeYoe and Sisola, 1991; Van Essen et al., 1991). V4 was initially characterized as a color-processing area, but subsequent studies revealed that it contains a diverse complement of cells, including those with preferences for color, orientation, and disparity, as well as higher order feature preferences. V4 also appears to have a modular organization (DeYoe and Sisola, 1991; DeYoe

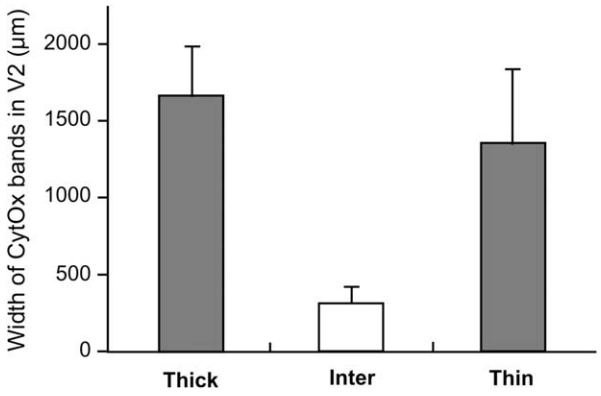

Figure 9. Width of the CytOx modules of V2. Frequency histogram of the mean and SD of the widths of CytOx-rich thin and thick bands and CytOx-poor interbands of V2.

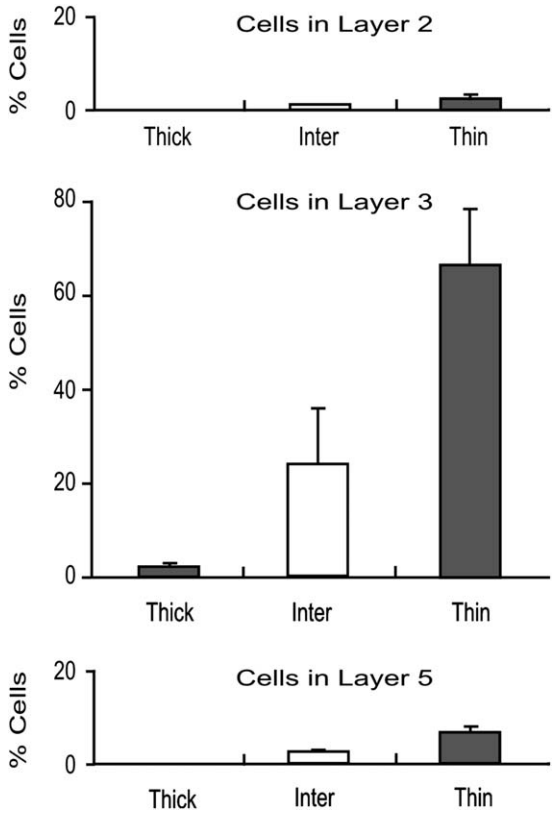

Figure 10. Distribution of cells in CytOx modules and cortical layers. Mean relative frequency of cells in layers II, III, and V of V2 after injections of CTb into V4. Whiskers represent 1 SD.

et al., 1994; Yoshioka et al., 1992); the geometry of the modules and their relations to color and form analyses remain unclear. Tanigawa et al. (2010) suggested that V4 consists of multiple, alternating, band-like structures for color and orientation. Such band-like organization was also found in the pattern of afferent connections from V2 thin stripes and pale stripes (Xiao et al., 1999). More recently, Li et al. (2013) found that V4 even contains direction-preferring domains that are preferentially activated by stimuli moving in one direction, suggesting that, in contrast to the classical view, motion information is also processed in ventral pathway regions such as area V4. Although neurons within the stations along the occipitotemporal pathway appear to play a significant role in the analyses of color and form information, it should be emphasized that this pathway is not equivalent to the "parvo" system. First, the blobs in V1, which contribute to this pathway, receive magnocellular and parvocellular inputs (Lachica et al., 1992). Second, deactivations of both the magnocellular and parvocellular layers of the LGN affect the activity of V4 neurons (Ferrera et al., 1992). In *Cebus* monkeys, we found that the sources of the projections from V2 to V4 are located in the CytOx-rich thin stripes and CytOx-poor interstripe regions, which corroborates earlier reports in the macaque (Nakamura et al., 1993; Felleman et al., 1997).

Yau et al. (2013) revealed a dynamic transformation of shape information occurring in area V4. Such dynamics might reflect influences from earlier (V1, V2) and later (central and anterior IT) processing stages in the ventral pathway and reflect a sequential hierarchical process of shape synthesis.

Pan et al. (2012) suggested that V4 is also a key cortical locus for integration of local features into global contours for the representation of illusory contours that are achieved by a progressive integration of local cues through the reciprocal circuits of V1, V2, and V4, with V4 as a key player mediating the feedforward and feedback processing streams. In addition, according to Maunsell and Treue (2006), the existence of feature segregation in V4 would have significant implications for studies on the role of V4 in visual perception and feature-based attention. An understanding of the feedback and feedforward interplay between V2 and V4 is also important to an understanding of how attention modulates early stages of visual processing. Attentional influences have now been demonstrated throughout the visual cortex, and their influence on the processing of visual information is profound (Desimone, 1998). Reynolds et al. (2000) and Cohen and Maunsel (2011) have shown that attention increases sensitivity of V4 neurons.

Feedback and feedforward connections and laminar distribution

The laminar location of the cell bodies and terminals of interareal connections has been seen as a criterion

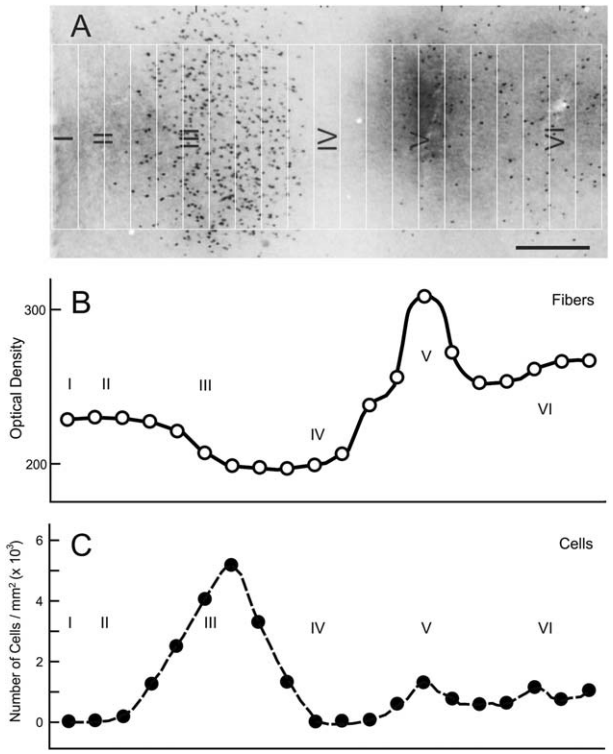

Figure 11. Variation in the numbers of labeled cells and the densities of fibers in different cortical layers through a CytOx-rich thin band of V2 after injection of CTb into V4. The density of labeled cells peaks in layer III (5 cells/mm^2), whereas the density of fibers is greater in layer V. The measurements were made in an oblique section divided into 21 rectangles of 534 × 70 μm. Scale bar = 200 μm.

for the hierarchical structural organization of the cortex and has been intensively studied. It has been proposed that feedforward projections from lower order cortical visual areas originate mainly in layer III and terminate predominantly in layer IV, whereas feedback projections from higher order areas to lower order areas originate mainly in layers V and VI and avoid layer IV by terminating above and below layer IV (Rockland and Pandya, 1979; Tigges et al., 1981; Maunsell and Van Essen, 1983; Markov et al., 2014). Maunsell and Van Essen have also described an additional anterograde projection pattern that they termed intermediate because it was not clearly either feedforward or feedback; these intermediate-type connections are characterized by terminal patches that vary from one type to another or by terminals that are homogenously distributed across all layers, including layer IV, but they are not heaviest in layer IV. Supragranular layers contain highly segregated bottom-up and top-down streams, both of which exhibit point-to-point connectivity different from the infragranular layers, which contain diffuse bottom-up and top-down streams. They have also pointed out that feedforward pathways have higher weights, cross fewer hierarchical levels, and are less numerous than feedback pathways.

Using tritiated amino acids, Gattass et al. (1997) demonstrated that V2 projects topographically back to V1 and forward to V3, V4, and MT. Within area V1, heavy anterograde label was found in layers I and VI in most cases, and occasionally in layer IVb. In this previous study, anterograde labeling in the remainder of the areas was always heaviest in layer IV. Based on the distinctions mentioned above, Ungerleider et al. (2008) were able to categorize the connections of V4 in macaque as feedback, intermediate, or feedforward. In both V2 and V3, retrogradely labeled cells were located predominantly in the supragranular layers, and the anterogradely labeled terminals were located in layers I and VI and avoided layer IV. Our results in *Cebus* emphasize the origin of the V4 feedforward connections in layer III and identify the target of the feedback connections as the supra- and infragranular layers, but mainly layer V.

Information conveyed along the occipitotemporal pathway

In addition to the major anatomical routes into the temporal lobe, there are other, smaller, "side routes" whose significances are currently unclear. Two of the most intriguing side routes are the direct projection from the foveal representation of V1 to area V4 that bypasses V2 (Kuypers et al., 1965; Cragg and Ainsworth, 1969; Zeki, 1978; Yukie and Iwai, 1985; Steele et al., 1991), and the direct projection from V2 to TEO that bypasses V4 (Morel and Bullier, 1990; Baizer et al., 1991; Distler et al., 1993; Weller and Steele, 1992). These bypass pathways may allow for a certain amount of parallel processing across the areas of the occipitotemporal projection system.

The intermingling of V2 cells projecting to areas V4 and TEO suggests that similar information is relayed to both areas. Although there is still some question about the relative proportions of color- and orientation-selective cells in the CO-rich thin stripes and CO-poor interstripe regions of V2, it is commonly accepted that these two stripe systems, taken together, contain many color- and form-selective cells and some cells that are selective for both (Livingstone and Hubel, 1984; DeYoe and Van Essen, 1985; Hubel and Livingstone, 1985, 1987). The thin stripe and interstripe regions lack large numbers of directionally selective cells, which instead are mainly located in the CO-rich thick stripes that project to area MT (DeYoe and Van Essen, 1985; Shipp and Zeki, 1985; Hubel and Livingstone, 1987).

CONCLUSIONS

We found that the sources of the projections from V2 to V4 are located in the CytOx-rich thin stripes and CytOx-poor interstripe regions, which confirms earlier reports (Nakamura et al., 1993; Felleman et al., 1997; Nascimento-Silva et al., 2003). Although some authors have reported some intermingling between the visual pathways (Sincich and Horton, 2005; Nassi and Callaway, 2006; Nassi et al., 2006; Ninomiya et al., 2011), our data reinforce the idea that some degree of segregation seems to be maintained between the dorsal and ventral streams. So, the parallel inputs from the LGN can be recombined in areas V1 and V2, where the dorsal and ventral streams originate, and conveyed to areas MT and PO as well as other parietal areas for the processing of motion and depth and to V4 and IT for the processing of form and color (Gattass et al., 2005; Orban, 2008; Nassi and Callaway, 2009). We also found that the majority of feedforward projections were from pyramidal cells with ascending dendrites located predominantly in the supragranular layers and sparsely in the infragranular layers, whereas the feedback projections (i.e., terminal-like labels) were located in the supra- and infragranular layers.

ACKNOWLEDGMENTS

We thank E. Saturato da Silva, L. Heringer, and T. Monteiro for technical help.

CONFLICT OF INTEREST STATEMENT

We declare that there is no conflict of interest, in the form of either financial, personal, or other relationships with other people or organizations within 3 years of beginning the submitted work that could inappropriately influence the results or interpretation of the data of the manuscript.

ROLE OF AUTHORS

All authors had full access to all the data in the study and take responsibility for the integrity of the data and the accuracy of the data analysis. Study concept and design: SNS, RG. Acquisition of data: SNS, RG, JGMS, CP. Analysis and interpretation of data: SNS, RG, JGMS. Drafting of the manuscript: SNS. Critical revision of the manuscript for important intellectual content: RG, JGMS, CP. Statistical analysis: SNS. Obtained funding: RG. Study supervision: RG.

LITERATURE CITED

An X, Gong H, Qian L, Wang X, Pan Y, Zhang X, Yang Y, Wang W. 2012. Distinct functional organizations for processing different motion signals in V1, V2, and V4 of macaque. J Neurosci 32:13363–13379.

Angelucci A, Clascá F, Sur M. 1996. Anterograde axonal tracing with the subunit B of cholera toxin: a highly sensitive immunohistochemical protocol for revealing fine axonal morphology in adult and neonatal brains. J Neurosci Methods 65:101–112.

Baizer JS, Ungerleider LG, Desimone R. 1991. Organization of visual inputs to the inferior temporal and posterior parietal cortex in macaques. J Neurosci 11:168–l90.

Boussaoud D, Desimone R, Ungerleider LG. 1991. Visual topography of area TEO in the macaque. J Comp Neurol 306:554–575.

Carroll EW, Wong-Riley MTT. 1984. Quantitative light and electron microscopic analysis of cytochrome oxidase-rich zones in the striate cortex of the squirrel monkey. J Comp Neurol 222:1–17.

Cohen MR, Maunsell JHR. 2011. Using neuronal populations to study the mechanisms underlying spatial and feature attention. Neuron 70:1192–1204.

Cragg BG, Ainsworth A. 1969. The topography of the afferent projections in the circumstriate visual cortex of the monkey studied by the Nauta method. Vision Res 9:733–747.

Cusick CG, Kaas JH. 1988. Cortical connections of area 18 and dorsolateral visual cortex in squirrel monkeys. Visual Neurosci 1:211–237.

Desimone R. 1998. Visual attention mediated by biased competition in extrastriate visual cortex. Philos Trans R Soc Lond B 353:1245–1255.

Desimone R, Gross CG. 1979. Visual areas in the temporal cortex of the macaque. Brain Res 178:363–380.

Desimone R, Schein SJ. 1987. Visual properties of neurons in area V4 of the macaque: sensitivity to stimulus form. J Neurophysiol 57:835–868.

Desimone R, Ungerleider LG. 1989. Neural mechanisms of visual processing in monkeys. In: Boller F, Grafman J, editors. Handbook of neuropsychology, vol 2. Amsterdam: Elsevier. p 267–299.

Desimone R, Schein SJ, Moran J, Ungerleider LG. 1985. Contour, color, and shape analysis beyond the striate cortex. Vision Res 25:441–452.

Desimone R, Moran J, Schein SJ, Mishkin M. 1992. A role for the corpus callosum in visual area V4 of the macaque. Visual Neuroci 10:159–171.

DeYoe EA, Sisola LC. 1991. Distinct pathways link anatomical sub-divisions of V4 with V2 and temporal cortex in the macaque monkey. Soc Neurosci Abstr 17:1282.

DeYoe EA, Van Essen DC. 1985. Segregation of efferent connections and receptive field properties in visual area V2 of the macaque. Nature 317:58–61.

DeYoe EA, Felleman DJ, Van Essen DC, McClendon E. 1994. Multiple processing streams in occipitotemporal visual cortex. Nature 371:151–154.

Distler C, Boussaoud D, Desimone R, Ungerleider LG. 1993. Cortical connections of inferior temporal area TEO in macaque monkeys. J Comp Neurol 334:125–150.

Federer F, Ichida JM, Jeffs J, Schiessl I, McLoughlin N, Angelucci A. 2009. Four projection streams from primate V1 to the cytochrome oxidase stripes of V2. J Neurosci 29:15455–15471.

Federer F, Williams D, Ichida JM, Merlin S, Angelucci A. 2013. Two projection streams from macaque V1 to the pale cytochrome oxidase stripes of V2. J Neurosci 33:11530–11539.

Felleman DJ. 2008. Functional maps in visual cortex: Topographic, modular, and column organizations. In: Masland RH, Albright TA, editors. The senses. London: Elsevier. p 577–593.

Felleman DJ, Van Essen DC. 1991. Distributed hierarchical processing in the primate cerebral cortex. Cereb Cortex 1:1–47.

Felleman DJ, Xiao Y, McClendon E. 1997. Modular organization of occipito-temporal pathways: cortical connections between visual area 4 and visual area 2 and posterior inferotemporal ventral area in macaque monkeys. J Neurosci 17:3185–3200.

Ferrera VP, Nealey TA, Maunsell JHR. 1992. Mixed parvocellular and magnocellular geniculate signals in visual area V4. Nature 358:756–758.

Gattass R, Gross CG, Sandell JH. 1981. Visual topography of V2 in the macaque. J Comp Neurol 201:519–530.

Gattass R, Sousa APB, Covey E. 1985. Cortical visual areas of the macaque: possible substrates for pattern recognition mechanisms. In: Chagas C, Gattass R, Gross CG, editors. Pattern recognition mechanisms Vatican City: Pontifical Academy of Sciences. p 1–20.

Gattass R, Sousa APB, Gross CG. 1988. Visuotopic organization and extent of V3 and V4 of the macaque. J Neurosci 8:1831–1845.

Gattass R, Rosa MGP, Sousa APB, Piñon MCG, Fiorani M Jr, Neuenschwander S. 1990. Cortical streams of visual information processing in primates. Braz J Med Biol Res 23:375–393.

Gattass R, Sousa AP, Mishkin M, Ungerleider LG. 1997. Cortical projections of area V2 in the macaque. Cereb Cortex 7:110–129.

Gattass R, Nascimento-Silva S, Soares JG, Lima B, Jansen AK, Diogo AC, Farias MF, Botelho MM, Mariani OS, Azzi J, Fiorani M. 2005. Cortical visual areas in monkeys: location, topography, connections, columns, plasticity and cortical dynamics. Philos Trans R Soc Lond B 360:709–731

Gross CG, Rocha-Miranda CE, Bender DB. 1972. Visual properties of neurons in inferotemporal cortex of the macaque. J Neurophysiol 35:96–111.

Horton JC. 1984. Cytochrome oxidase patches: a new cytoarchitectonic feature of macaque visual cortex. Philos Trans R Soc Lond B 304:199–253.

Horton JC, Hubel DH. 1981. Regular patchy distribution of cytochrome oxidase staining in primate visual cortex of macaque monkey. Nature 292:762–764.

Hubel DH, Livingstone MS. 1985. Complex-unoriented cells in a subregion of primate area 18. Nature 315:325–327.

Hubel DH, Livingstone MS. 1987. Segregation of form, color, and stereopsis in primate area 18. J Neurosci 7:3378–3415.

Humphrey AL, Hendrickson AE. 1983. Background and stimulus-induced patterns of high metabolic activity in the visual cortex (area 17) of the squirrel and macaque monkey. J Neurosci 3:345–358.

Kaskan PM, Lu HD, Dillenburger BC, Kaas JH, Roe AW. 2009. The organization of orientation-selective, luminance-change and binocular-preference domains in the second (V2) and third (V3) visual areas of New World owl monkeys as revealed by intrinsic signal optical imaging. Cereb Cortex 19:1394–1407.

Kravitz DJ, Saleem KS, Baker CI, Mishkin M. 2011. A new neural framework for visuospatial processing. Nat Rev Neurosci 12:217–230.

Krubitzer L, Kaas J. 1990. Convergence of processing channels in the extrastriate cortex of monkeys. Visual Neuroci 5:609–613.

Kuypers HG, Szwarcbart MK, Mishkin M, Rosvold HE. 1965. Occipitotemporal corticocortical connections in the rhesus monkey. Exp Neurol 11:245–262.

Lachica EA, Beck PD, Casagrande VA. 1992. Parallel pathways in macaque monkey striate cortex: anatomically defined columns in layer III. Proc Natl Acad Sci U S A 89:3566–3570.

Levitt JB, Kiper DC, Movshon JA. 1994. Receptive fields and functional architecture of macaque V2. J Neurophysiol 71:2517–2542.

Li P, Zhu S, Chen M, Han C, Xu H, Hu J, Fang Y, Lu HD. 2013. A motion direction preference map in monkey V4. Neuron 78:376–388.

Lim H, Wang Y, Xiao Y, Hu M, Felleman DJ. 2009. Organization of hue selectivity in macaque V2 thin stripes. J Neurophysiol 102:2603–2615.

Livingstone MS, Hubel DH. 1982. Thalamic inputs to cytochrome oxidase-rich regions in monkey visual cortex. Proc Natl Acad Sci U S A 79:6098–6101.

Livingstone MS, Hubel DH. 1984. Anatomy and physiology of a color system in the primate visual cortex. J Neurosci 4: 309–356.

Livingstone MS, Hubel DH. 1987. Connections between layer 4B of area 17 and the thick cytochrome oxidase stripes of area 18 in the squirrel monkey. J Neurosci 7:3371–3377.

Lu HD, Roe AW. 2007. Optical imaging of contrast response in Macaque monkey V1 and V2. Cereb Cortex 17:2675–2695.

Lu HD, Roe AW. 2008. Functional organization of color domains in V1 and V2 of macaque monkey revealed by optical imaging. Cereb Cortex 18:516–33.

Lu HD, Chen G, Tamogawa H, Roe AW. 2010. A motion direction map in macaque V2. Neuron 68:1002–1013.

Markov NT, Vezoli J, Chameau P, Falchier A, Quilodran R, Huissoud C, Lamy C, Misery P, Giroud P, Ullman S, Barone P, Dehay C, Knoblauch K, Kennedy H. 2014. Anatomy of hierarchy: feedforward and feedback pathways in macaque visual cortex. J Comp Neurol 522:225–259.

Maunsell JH, Newsome WT. 1987. Visual processing in monkey extrastriate cortex. Annu Rev Neurosci 10:363–401.

Maunsell JH, Treue S. 2006. Feature-based attention in visual cortex. Trends Neurosci 29:317–322.

Maunsell JH, Van Essen DC. 1983. The connections of the middle temporal visual area (MT) and their relationship to a cortical hierarchy in the macaque monkey. J Neurosci 3:2563–2586.

Mishkin M, Ungerleider LG, Macko KA. 1983. Object vision and spatial vision: two cortical pathways. Trends Neurosci 414–417.

Morel A, Bullier J. 1990. Anatomical segregation of two cortical visual pathways in the macaque monkey. Visual Neuroci 4:555–578.

Nakamura H, Gattass R, Desimone R, Ungerleider LG. 1993. The modular organization of projections from areas V1 and V2 to areas V4 and TEO in macaques. J Neurosci 13:3681–3691.

Nascimento-Silva S, Gattass R, Fiorani M Jr, Sousa APB. 2003 Three streams of visual information processing in V2 of Cebus monkey. J Comp Neurol 466:104–118.

Nassi JJ, Callaway EM. 2006. Multiple circuits relaying primate parallel visual pathways to the middle temporal area. J Neurosci 26:12789–12798.

Nassi JJ, Callaway EM. 2009. Parallel processing strategies of the primate visual system. Nat Rev Neurosci 10:360–372.

Nassi JJ, Lyon DC, Callaway EM. 2006. The parvocellular LGN provides a robust disynaptic input to the visual motion area MT. Neuron 50:319–327.

Ninomiya T, Sawamura H, Inoue K, Takada M. 2011. Differential architecture of multisynaptic geniculo-cortical pathways to V4 and MT. Cereb Cortex 21:2797–2808.

Orban GA. 2008 Higher order visual processing in macaque extrastriate cortex. Physiol Rev 88:59–89.

Pan Y, Chen M, Yin J, An X, Zhang X, Lu Y, Gong H, Li W, Wang W. 2012. Equivalent representation of real and illusory contours in macaque V4. J Neurosci 32:6760–70.

Pasupathy A, Connor CE. 1999. Responses to contour features in macaque area V4. J Neurophysiol 82:2490–2502.

Reynolds JH, Pasternak T, Desimone R. 2000. Attention increases sensitivity of V4 neurons. Neuron 26:703–714

Rockland KS, Pandya DN. 1979. Laminar origins and terminations of cortical connections of the occipital lobe in the rhesus monkey. Brain Res 179:3–20

Rosa MGP, Souza APB, Gattass R. 1988. Representation of the visual field in the second visual area in the Cebus monkey. J Comp Neurol 275:326–345.

Schein SJ, Desimone R. 1990. Spectral properties of V4 neurons in the macaque. J Neurosci 10:3369–3389.

Shipp S, Zeki S. 1985. Segregation of pathways leading from area V2 to areas V4 and V5 of macaque monkey visual cortex. Nature 315:322–325.

Shipp S, Zeki S. 1989. The organization of connections between areas V5 and V2 in macaque monkey visual cortex. Eur J Neurosci 1:333–354.

Shipp S, Adams DL, Moutoussis K, Zeki S. 2009. Feature binding in the feedback layers of area V2. Cereb Cortex 19:2230–2239.

Silverman MS, Tootell RBH. 1987. Modified technique for cytochrome oxidase histochemistry increased staining intensity and compatibility with 2-deoxyglucose autoradiography. J Neurosci Methods 19:1–10.

Sincich LC, Horton JC. 2005. Input to V2 thin stripes arises from V1 cytochrome oxidase patches. J Neurosci 25: 10087–10093.

Sincich LC, Jocson CM, Horton JC. 2010. V1 interpatch projections to V2 thick stripes and pale stripes. J Neurosci 30:6963–6974.

Sousa AP, Piñon MCG, Gattass R, Rosa MPG. 1991. Topographic organization of cortical input to striate cortex in the *Cebus* monkey: a fluorescent tracer study. J Comp Neurol 308:665–682.

Spatz WB, Tigges J. 1972. Experimental-anatomical studies on the "middle temporal visual area (MT)" in primates. I. Efferent cortico-cortical connections in the marmoset *Callithrix jacchus*. J Comp Neurol 146:451–464.

Steele GE, Weller RE, Cusick CC. 1991. Cortical connections of the caudal subdivision of the dorsal area (V4) in monkeys. J Comp Neurol 306:495–520.

Tanaka K, Saito H, Fukuda Y, Moriya M. 1991. Coding visual images of objects in the inferotemporal cortex of the macaque monkey. J Neurophysiol 66:170–189.

Tanigawa H, Lu HD, Roe AW. 2010. Functional organization for color and orientation in macaque V4. Nat Neurosci 13:1542–1548.

Tigges J, Tigges M, Anschel S, Cross NA, Letbetter WD, McBride RL. 1981. Areal and laminar distribution of neurons interconnecting the central visual cortical areas 17, 18, 19 and MT in the squirrel monkey (*Saimiri*). J Comp Neurol 202:539–550.

Tootell RBH, Silverman MS, De Valois RL, Jacobs GH. 1983. Functional organization of the second cortical visual area in primates. Science 220:737–739.

Ungerleider LG. 1985. The corticocortical pathways for object recognition and spatial perception. In: Chagas C, Gattass R, Gross CG, editors. Pattern recognition mechanisms. Vatican City: Pontifical Academy of Sciences. p 21–37.

Ungerleider LG, Desimone R. 1986. Cortical connections of visual area MT in the macaque. J Comp Neurol 248:190–222.

Ungerleider LG, Mishkin M. 1982. Two cortical visual svstems. In: Ingle DJ, Goodale MA, Mansfield RJW, editors. Analysis of visual behavior. Cambridge, MA: MIT Press. p 549–586.

Ungerleider LG, Galkin TW, Desimone R, Gattass R. 2008. Cortical connections of area V4 in the macaque. Cereb Cortex 18:477–499.

Van Essen DC, Felleman DJ, DeYoe EA, Olavania J, Knierim JJ. 1991. Modular and hierarchical organization of extrastriate visual cortex in the macaque monkey. Cold Spring Harbor Symp Quant Biol 55:679–696.

Van Essen DC, Anderson CH, Felleman DJ. 1992. Information processing in the primate visual system: an integrated systems perspective. Science 2554:19–423.

Weller RE. 1988. Two cortical visual systems in old world and new world primates. In: Hicks TP, Benedek G, editors. Progress in brain research, vol75. Amsterdam: Elsevier. p 293–306.

Weller RE, Kaas JH. 1985. Cortical projections of the dorsolateral visual area in owl monkeys: the prestriate relay to inferior temporal cortex. J Comp Neurol 234:35–59.

Weller RE, Steele GE. 1992. Cortical connections of subdivisions of inferior temporal cortex in squirrel monkeys. J Comp Neurol 324:37–66.

Wong-Riley MTT, Carroll EW. 1984. Quantitative light and electron microscopic analysis of cytochrome oxidase-rich zones in V2 prestriate cortex of the squirrel monkey. J Comp Neurol 222:18–37.

Xiao Y, Zych A, Felleman DJ. 1999. Segregation and convergence of functionally defined V2 thin stripe and interstripe compartment projections to area V4 of macaques. Cereb Cortex 9:792–804.

Yau JM, Pasupathy A, Brincat SL, Connor, CE. 2013. Curvature processing dynamics in macaque area V4. Cereb Cortex 23:198–209.

Yoshioka T, Levitt JB, Lund JS. 1992. Intrinsic lattice connections of macaque monkey visual cortical area V4. J Neurosci 12:2785–2802.

Yukie M, Iwai E. 1985. Laminar origin of direct projection from cortex area V1 to V4 in the rhesus monkey. Brain Res 346:383–386.

Zeki SM. 1978. Uniformity and diversity of structure and function in rhesus monkey prestriate visual cortex. J Physiol 277:273–290.

Zeki SM, Shipp S. 1988. The functional logic of cortical connections. Nature 355:311–317.

Zeki SM, Shipp S. 1989. Modular connections between areas V2 and V4 of macaque monkey visual cortex. Eur J Neurosci 1:494–506.